

Differences of digital camera resolution metrology to describe noise reduction artifacts

Uwe Artmann^a and Dietmar Wueller^b

^{a,b}Image Engineering, Augustinusstrasse 9d, 50226 Frechen, Germany;

ABSTRACT

Noise reduction in the image processing pipeline of digital cameras has a huge impact on image quality. It may result in loss of low contrast fine details, also referred to as texture blur. Previous papers have shown, that the objective measurement of the statistical parameter kurtosis in a reproduction of white Gaussian noise with the camera under test correlates well with the subjective perception of these ramifications. To get a more detailed description of the influence of noise reduction on the image, we compare the results of different approaches to measure the spatial frequency response (SFR). Each of these methods uses a different test target, therefore we get different results in the presence of adaptive filtering. We present a study on the possibility to derive a detailed description of the influence of noise reduction on the different spatial frequency sub bands based on the differences of the measured SFR using several approaches. Variations in the underlying methods have a direct influence on the derived measurements, therefore we additionally checked for the differences of all used methods.

Keywords: image quality evaluation, texture, siemens star, resolution, spatial frequency response, modulation transfer function, kurtosis, MTF, SFR

1. INTRODUCTION

Resolution measurement on system level (including optics, sensor and signal processing) of digital cameras can be performed using different test targets that are reproduced by the device under test. In absence of adaptive, non-linear filtering the results of the underlying methods are close to each other but in presence of this filtering, the results differ depending on the used structures and methods. We propose to use these differences to describe the influence of the signal processing on the spatial domain of the image.

2. TEST SETUP

For this study, we have used images taken with real cameras, varying from D-SLR to mobile phone cameras. As the results are based on the influence of optics, sensor and signal processing, we made sure, that the first two components are static and just the signal processing changed. The device under test was mounted on a massive tripod and was not moved within one series of images. Using a reprographic illumination with halogen light filtered to daylight (D50), different test targets have been reproduced. Each target has been placed in the image center so variation over the image field had no influence on the results of each measurement. If possible, the lens was focussed on the target plane and was left unchanged throughout the test while replacing the target. If not possible, three or more images have been taken per set to get the "best of three" image.

In this setup, we reduced the influence of varying optical influence to a minimum. To force the camera to use a different signal processing, we changed the nominal sensitivity, stated as ISO speed in the settings of the device. All tests have been performed at ISO 100, ISO 400 and ISO 1600 (if available, otherwise using the device specific setting). As with increasing ISO speed the exposure time is decreased, the signal to noise ratio on sensor level is reduced which results in an increased noise cleaning in the signal processing. As sharpening may influence the noise appearance in most cameras the sharpening also depends on the sensitivity level.

If all other components are fixed, the differences in the result of the resolution measurement approaches are direct related to the signal processing and can be used to describe it and its influence on the image. As a reference, we implemented a very simple processing with no noise reduction or sharpening applied to the image using the RAW file format and dcrw.¹⁰

Further author information: (Send correspondence to Uwe Artmann)

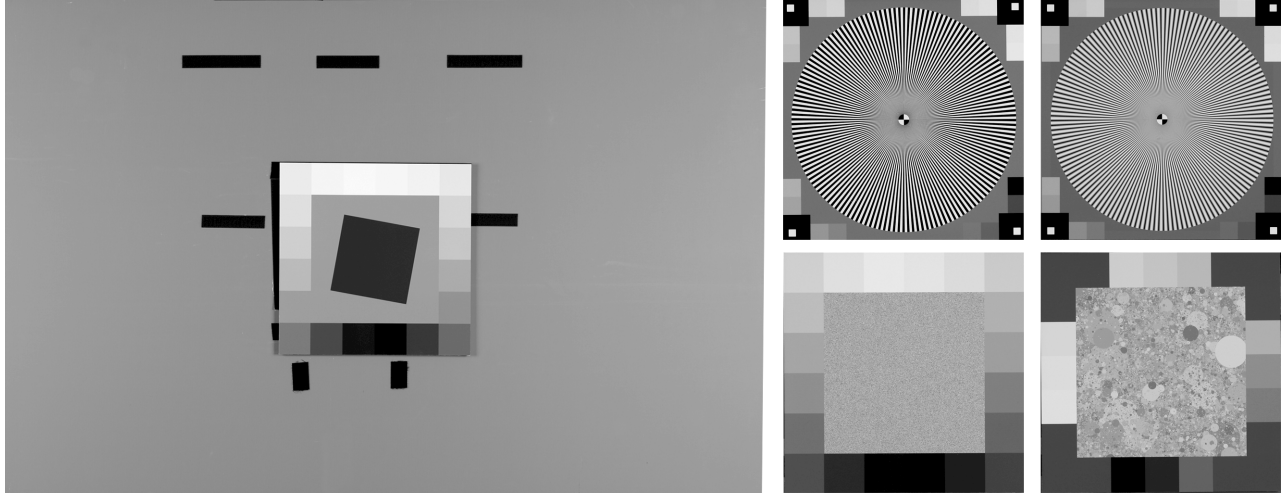


Figure 1. The target for the camera under test. The structure in the center was replaced one after the other, while the complete setup was left unchanged. *large*: Slanted Edge *top left*: bitonal siemens star *top right*: sinusoidal siemens star *bottom left*: gaussian noise *bottom right*: dead leaves model

3. RESOLUTION MEASUREMENT METHODS

The current version of the ISO standard 12233⁷ shows some problems due to the high contrast in the used slanted edge and the subjective evaluation on the other structures.¹¹ The ISO working group already addressed this problem and will release a revision with three different metrology protocols in the near future.⁹ Two of these methods (SFR_Siemens and SFR_Edge) provide a Spatial Frequency Response (SFR). This function describes the modulation in the image depending on the spatial frequency in the target. On a sinusoidal target this function can also be called Modulation Transfer Function (MTF). In this paper, we use the SFR_Edge approach, SFR_Siemens in two different implementations and two methods based on the reproduction of randomly distributed structures in the target (gaussian noise and the dead leaves model).

All targets are surrounded by 12 to 20 gray patches of different reflectances. Combining the known reflectance and the mean digital value of each patch one can calculate the Opto Electronic Conversion function (OECF). The inverse of the OECF is used to linearize the image, so that the relation of digital value to reflectance becomes linear. Both methods using a siemens star additionally reduce all digital values, that the lowest reflectance in the target becomes zero so that with (2) we get a modulation of one for very low spatial frequencies.

3.1. SFR-Siemens_sinusoidal

This method uses a siemens star with a harmonic function depending on the angle φ , taking the center of the star as the base of the angle.⁵ (see Fig: 2) It provides a Modulation Transfer Function MTF which describes the loss of modulation depending on the spatial frequency $f_{spatial}$ (see Eq.(1) and (2)).

$$MTF(f_{spatial}) = \frac{Modulation_{image}(f_{spatial})}{Modulation_{target}(f_{spatial})} \quad (1)$$

$$Modulation = \frac{I_{max} - I_{min}}{I_{max} + I_{min}} = \frac{a + b - (a - b)}{a + b + (a - b)} = \frac{2b}{2a} = \frac{b}{a} \quad (2)$$

Uwe Artmann: E-mail: mail@uwe-artmann.de, Telephone: +49 2234 912141 www.image-engineering.de
 Dietmar Wueller.: E-mail: d.wueller@ivent.de, Telephone: +49 2234 912141

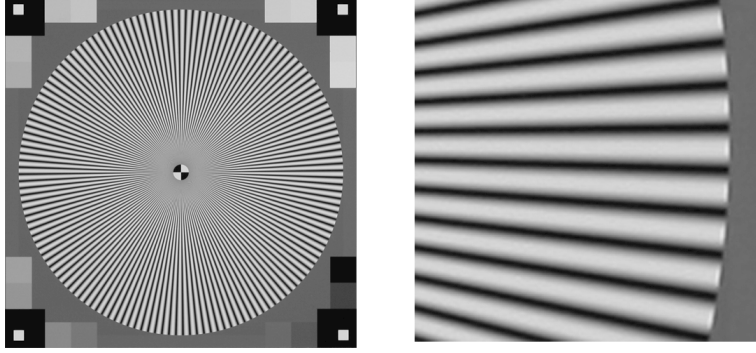


Figure 2. The test target used for the SFR-Siemens_sinusoidal approach *left*: complete chart *right*: Detail

It is part of the chart production to take care that the $Modulation_{target}(f_{spatial})$ is 1 for all frequencies used for the measurement. The intensity I in the ideal digital image as a reproduction of the chart is

$$I(\varphi) = a + b \cos\left(\frac{2\pi}{g}(\varphi - \varphi_0)\right) \quad (3)$$

with angle φ (4), period length g see (5), mean value a , amplitude b and phase φ_0 .

$$\varphi = \arctan\left(\frac{x}{y}\right) \text{ with } x, y = \text{projected coordinates in image} \quad (4)$$

$$g = \frac{\text{circumference [pixel]}}{\text{number of periods}} = \frac{2\pi r}{n_p} [\text{pixel}] \quad (5)$$

The image that shows the siemens star is acquired in and linearized, using the gray patches arranged around the star. The aim is to obtain the modulation depending on the spatial frequency that is defined by the radius r . The image coordinates are projected to the star coordinates, that sets the center of the star to $x=0$ and $y=0$. The star is subdivided into 24 segments to provide information on orientation specific differences. The modulation is obtained depending on three variables: radius r and the starting and ending angle φ_{start} and φ_{end}

The base for the calculation is the function $I(r, \varphi)$ which is directly read out of the image data. The pixels that are located best to the ideal circle with radius r are used to build up the 1D data-array.

After the reading for one radius r the row vector $I(\varphi)$ and the row vector φ are known. Using (3) the unknown variables are the phase φ_0 and a and b . To get the phase out of the calculation the approximation (6) is used instead of (3).

$$I(\varphi) = a + b_1 \sin\left(\frac{2\pi}{g}(\varphi)\right) + b_2 \cos\left(\frac{2\pi}{g}(\varphi)\right) \quad (6)$$

The mean a and the amplitude b_1 and b_2 are calculated using the least square error fit method that fits an idealized harmonic function to the obtained image intensity data. With the geometric mean of b_1 and b_2 the modulation is calculated as mentioned in (2). So the output of the calculation is the function $M(f, \varphi_{start}, \varphi_{end})^*$. So the output are up to 24 MTFs for each star in the image.

3.2. SFR-Siemens_bitonal

This approach also uses a siemens star as test target, but in this case the star is created by a rectangular function instead of a harmonic function of the angle. The algorithm for reading the image information is the same as for the SFR-Siemens_sinusoidal approach, so the the function $I(r, \varphi)$ which is directly read out of the image

*Modulation depending on spatial frequency f , starting angle φ_{start} and ending angle φ_{end}

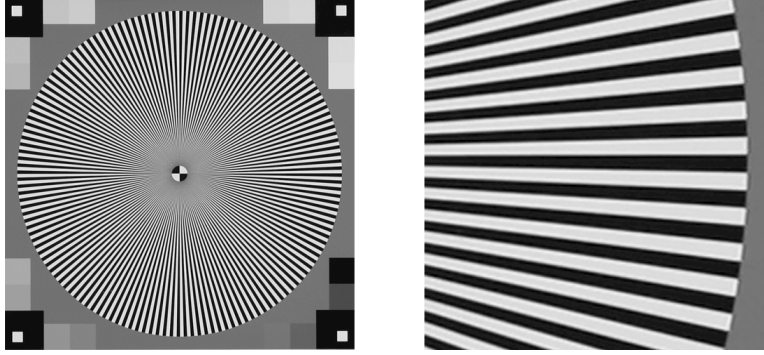


Figure 3. The test target used for the SFR-Siemens-bitonal approach *left: complete chart right: Detail*

data, is the base for the approach. Similar is the problem to detect the phase of the rectangular function. We implemented a brute force method to detect the phase. A generated rectangular function with the frequency related to r is correlated to the image data in $I(r, \varphi)$. So for all r and for a specific range of φ a correlation function is generated by shifting the generated function step by step and calculating the correlation coefficient. The higher this value, the better the shifted generated function fits the image data. The maximum of the correlation function provides the best fit, so the phase is now known.

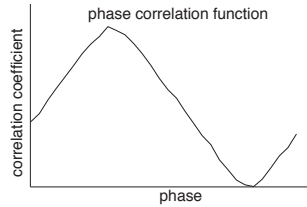


Figure 4. For each phase a correlation coefficient is calculated. The higher this value, the better the phase of the generated rectangular function matches the found pixel values.

If the phase is known, we can decide which value $I(r, \varphi)$ is related to a white area in the target and which value is related to the black area in the target. So for each radius r , we calculate I_{max} as the mean value of $I(r, \varphi)$ with all φ related to white in the target and I_{min} accordingly with φ related to black in the target. With I_{max} and I_{min} we calculate the modulation using (7).

$$Modulation = \frac{I_{max} - I_{min}}{I_{max} + I_{min}} \quad (7)$$

3.3. SFR-Edge

The SFR-Edge algorithm is described in ISO12233 and is based on the reproduction of a slanted edge in the image field. In this study, we used a slanted gray square, surrounded by a gray background. The modulation of square to background is 60%, as it could be shown^{6,1} that the contrast in the edge should not be too high to avoid saturation or dark subtraction effects on the result and not too low to reduce the influence of noise on the results.

The first step is to localize the edge in each row. Using this data, the offset and the slope of the edge in the image is calculated. The edge description is used to calculate an over-sampled pixel row. This is done by a binning process, placing each pixel of the image into a bin which describes a certain distance to the fitted edge. So the two-dimensional position of each pixel with column x and row y becomes a one-dimensional description with its distance to the edge. (see Fig. 6)

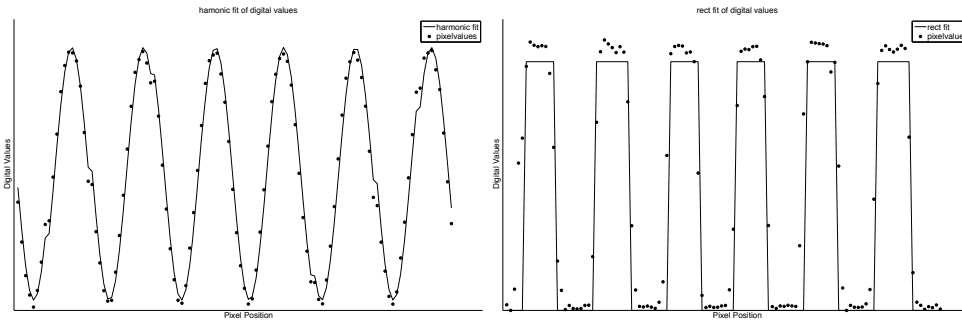


Figure 5. Visualization of the SFR-Siemens_sinusoidal and the SFR-Siemens_bitonal approach. *left*: a harmonic function is fitted into the pixel values along a defined radius for one segment *right*: a rectangular function with the best correlation coefficient is used to extract the position of all pixel values related to the white area in the target.

The over-sampled description of the edge is called the edge spread function *ESF*. The first derivative of the ESF is the line spread function *LSF*[†]. The SFR-Edge is the Fourier transform of the LSF. Before the transformation, the data is windowed to avoid leakage. (see Fig. 7)

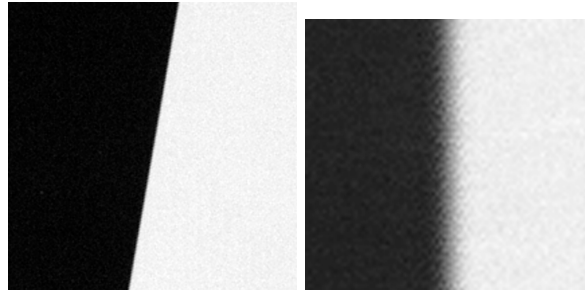


Figure 6. Basic concept of the SFR_Edge approach: The device under test reproduces a slanted edge (*left*, detail). All pixel values are rearranged according to their distance to the detected edge. The result is an over sampled representation of the edge, the mean value for each column leads to the edge spread function. (*right*, enlarged)

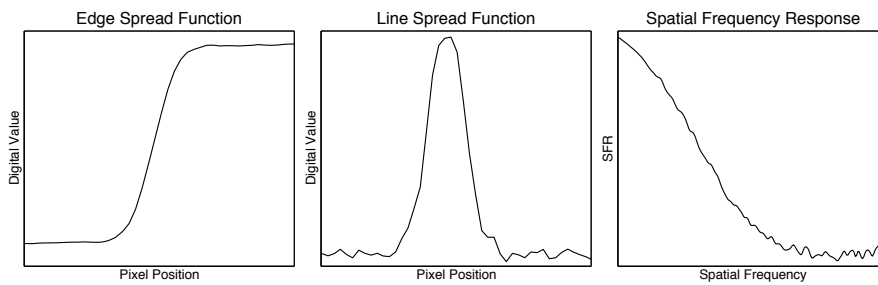


Figure 7. Basic concept of the SFR_Edge approach: The edge spread function is the over sampled intensity function of the edge. The derivative of this function is the line spread function. Transferred to the fourier spatial frequency domain, it is the spatial frequency response.

[†]The LSF can be imagined as a 1-D representative of the point-spread function PSF

3.4. Gaussian Power Spectrum

While the methods based on a siemens star completely stay in the spatial domain and measure each frequency "one-after-another", this approach measures completely in the frequency domain. The target is a random distribution of different reflectances that results in a gaussian distribution with a variance of 1/32. Seeing the camera as a system that needs to be characterized, the input to this system is a white, gaussian noise. A white noise contains all possible frequencies in the same power, like a light spectrum with all frequencies results into white light. Now the output of the system is checked for its spectral content, which represents the transfer function of the system. So if high spatial frequencies in the target can not be reproduced by any reason, this results in a lower content of high frequencies in the output. In the examples in Figure 8 one can see the differences in the image depending on different level of noise cleaning.

In our implementation, we calculate the magnitude spectrum for each row of a cut out in size $N * N^{\ddagger}$ of the image showing the noise. The average over all magnitude spectra is normalized and plotted in the frequency range of 0.01 to 0.5 cycles per pixel.

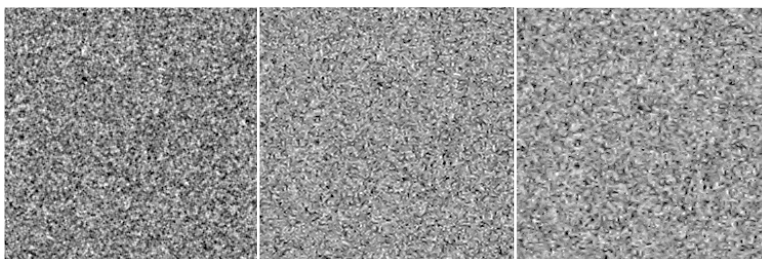


Figure 8. Comparison of reproduced white gaussian noise, using a D-SLR *left:* ISO100, basic RAW processing *center:* ISO100, JPEG *right:* ISO1600, JPEG *all:* leveled, enlarged 4x, nearest neighbor

3.5. Dead Leaves Texture MTF

Mobile phone camera modules are very limited in their image quality by size and cost constraints. Image processing is performed on these images to compensate for that, which results into the loss of low contrast fine detail (so called texture blur). To measure this effect, the I3A Camera Phone Image Quality working group¹² evaluates different approaches.³ One proposal is to use the statistical value of kurtosis as an indicator to set the values of noise and resolution measurement into perspective of noise reduction artefacts.² Another approach is based on a target that follows the dead leaves model proposed by Cao, Guichard and Hornung.⁴ It is based on a camera system model that assumes that the power spectrum PS of the image is the product of the power spectrum of the target and the system (8). The PS_{system} includes the complete chain of image generation (optics, sensor and signal processing).

$$PS_{image} = PS_{target} * PS_{system} \quad (8)$$

The target as shown in the examples in figure 9 very closely follows a power law. With the known power spectrum of the target PS_{target} and the measured power spectrum in the image PS_{image} , the so called "Dead Leaves MTF" is calculated as

$$DeadLeavesMTF = \frac{PS_{image}}{PS_{target}} \quad (9)$$

[‡] $N = 2^n$ with $n = 6, 7, 8, 9, ..$

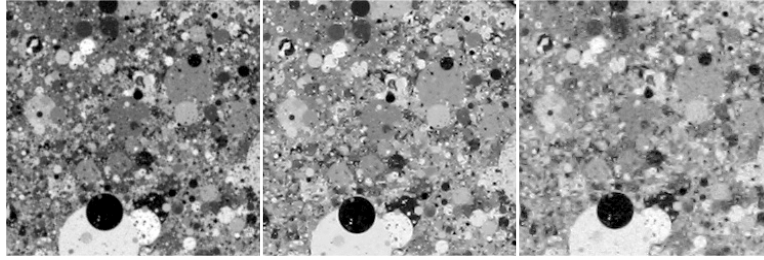


Figure 9. Comparison of the reproduced dead leaves chart, using a D-SLR *left*: ISO100, basic RAW processing *center*: ISO100, JPEG *right*: ISO1600, JPEG *all*: leveled, enlarged 4x, nearest neighbor

4. RESULTS

To compare the results of the different methods, we show the absolute results and the differences in one figure. For visualization, the differences are based on a polynomial fit of degree 6 of the results.

As a reference check, we build a very basic image pipeline. The RAW files from a D-SLR were converted to a 16bit Tiff File using ddraw. The images were demosaiced using a gradient-corrected linear interpolation and white balanced using a "gray world" approach. The result is a linear image file, that has no sharpening and no noise reduction applied. So comparing the results based on the images taken at ISO100 and ISO1600, the only difference is, that we have more noise in the second image.

4.1. Influence of Noise on Results

As shown in Figure 10, the results of all five implemented methods are very close to each other at ISO100. With the increased camera noise level at ISO1600, we see that the Dead Leaves MTF is highly influenced by this. This can be explained, by the missing noise component in (8). The camera system does add noise to the image, which has influence on the PS_{image} and as the PS_{target} is unchanged, this influence is shown in PS_{system} . We have the same effect in the Gaussian Power Spectrum method, but as the PS_{target} and the added noise spectrum are close to each other, the influence is lower and reduced by the normalization.

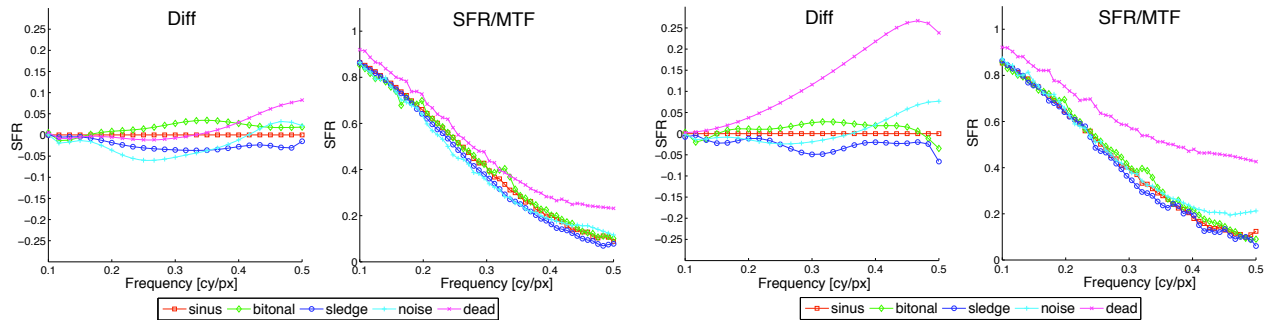


Figure 10. Comparison Canon 450D, basic RAW implementation *left*: ISO100 *right*: ISO1600

4.2. Influence of Denoising on Results

Figure 11 shows the influence of denoising on the results. The images have been denoised using an adaptive filter (Adobe Photoshop) to reduce the noise. One can see, that the differences between the different ISO speed settings are very low, so the influence of noise on the results disappeared. Measuring the target corrected power spectrum on the noise patch and on the dead leaves target provides a significant lower results than the other methods.

Both methods measuring in the spatial domain (both SFR-Siemens methods) show a gap at 0.125 and 0.25 cycles per pixel. This local loss of modulation can be observed in the image as well is not a measurement error. All other methods fail to show this effect.

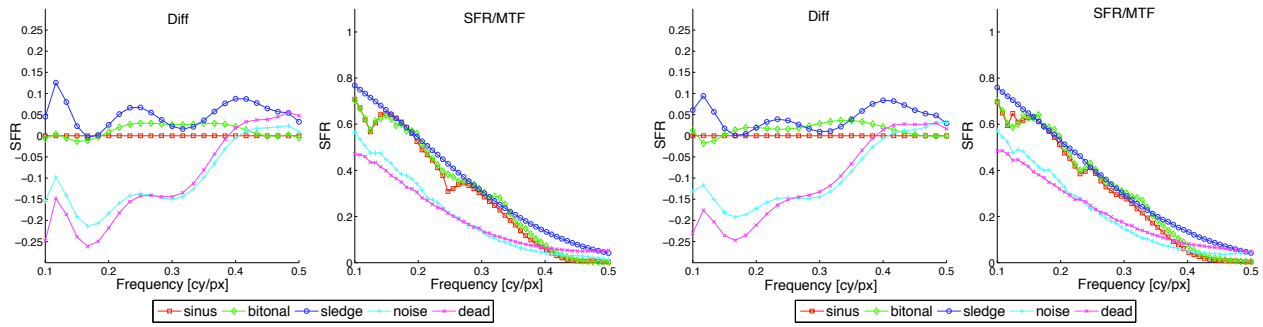


Figure 11. Comparison Canon 450D, basic RAW implementation, denoised, no sharpening *left: ISO100 right: ISO1600*

4.3. Influence of Sharpening on Results

We applied sharpening to the image (unsharp masking) and show the results in Figure 12. As the sharpening has a higher influence on edges than on other image content, we get significant differences between SFR-Siemens_sinusoidal and SFR-Siemens_bitonal and between the Gaussian Power Spectrum and Dead Leaves MTF results. As we use a medium contrast slanted edge, the differences between SFR-Edge and SFR-Siemens are low.

The differences between the results of the ISO 100 and the ISO 1600 image are low, expect for the Dead Leaves MTF which gets totally different shape. As we have seen in 4.1, the image noise has a significant impact on the results. This effect is even intensified by the sharpening.

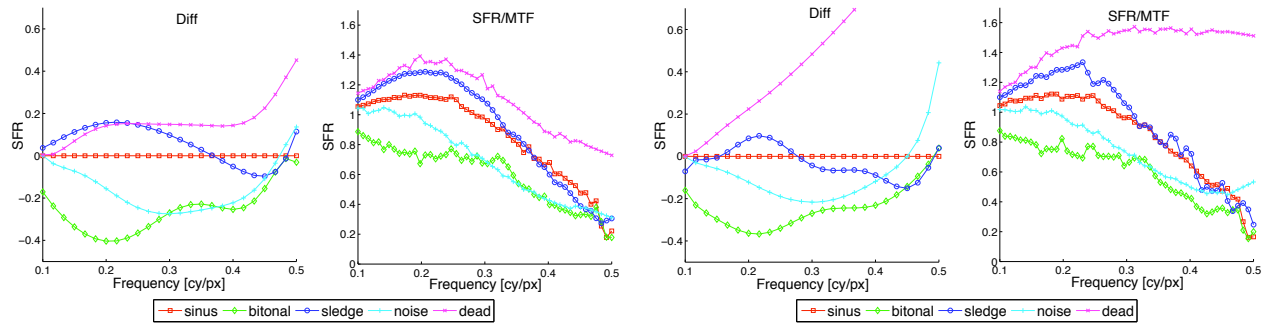


Figure 12. Comparison Canon 450D, basic RAW implementation, no denoising, sharpening *left: ISO100 right: ISO1600*

4.4. Influence of Denoising and Sharpening on Results

In another step, we combined denoising and sharpening, which would be the case for most camera applications. (Figure: 13) We also show the results of the standard JPEG processing in the same camera (Figure 14). In that case, one can see that the sharpening depends on the sensitivity setting in this camera observed in the changing results of SFR-Siemens and SFR-Edge. The difference of the denoising can be seen in the decreased results of Gaussian Power Spectrum and Dead Leaves MTF results.

4.5. Real Cameras

The complete amount of data that was produced can not be presented in this paper, but we picked some interesting results.

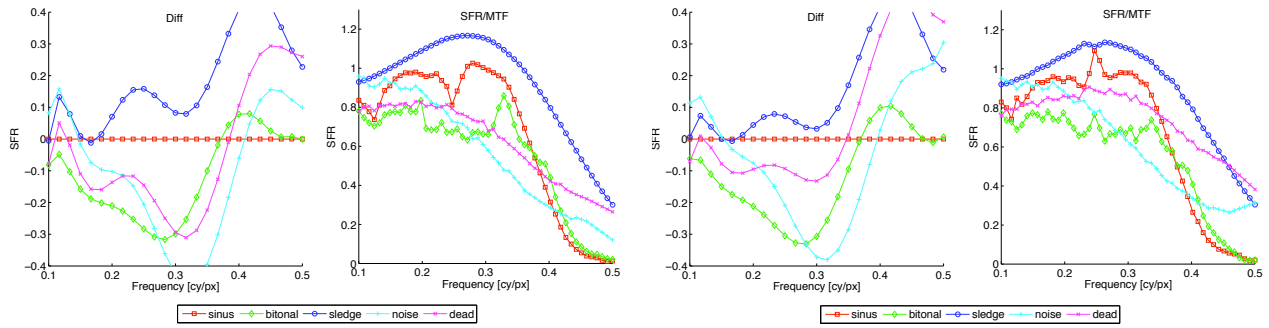


Figure 13. Comparison Canon 450D, basic RAW implementation, denoised, sharpening *left: ISO100 right: ISO1600*

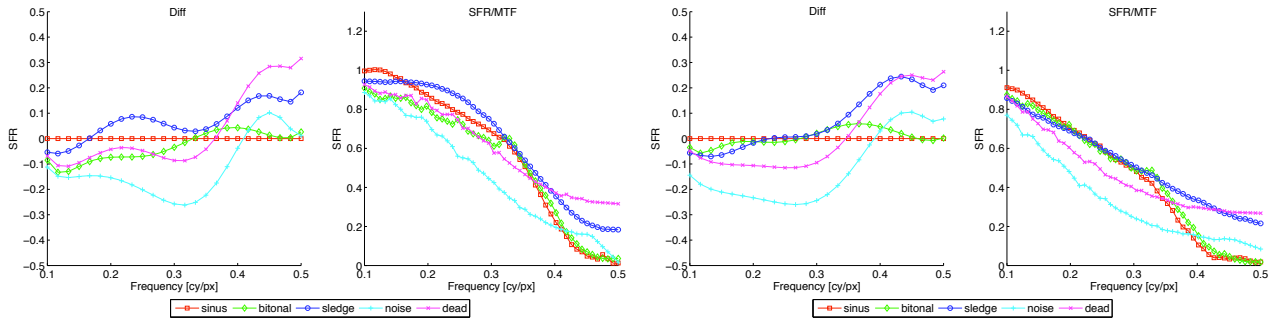


Figure 14. Comparison Canon 450D, JPEG *left: ISO100 right: ISO1600*

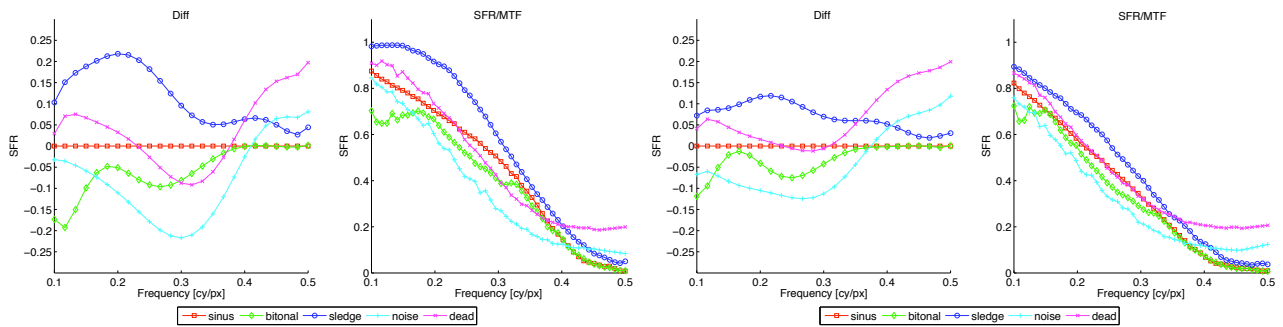


Figure 15. Comparison Nikon D300, JPEG *left: ISO100 right: ISO1600*

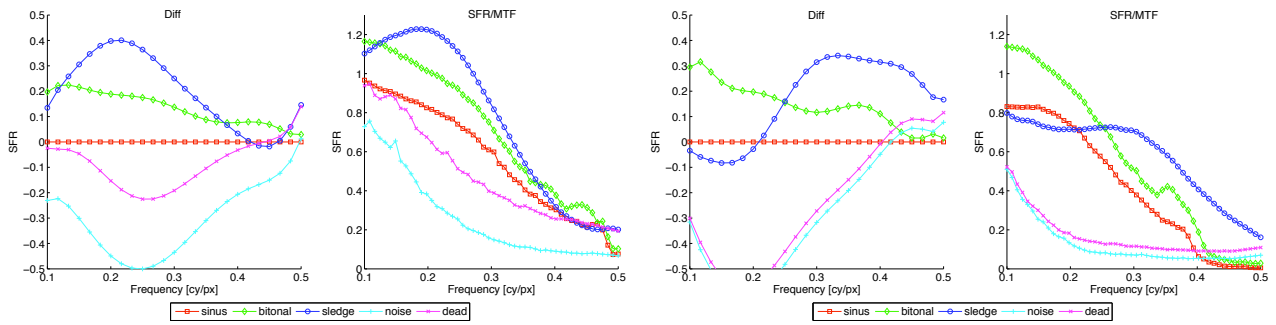


Figure 16. Comparison mobile phone, standard JPEG left: ISO100 right: ISO800

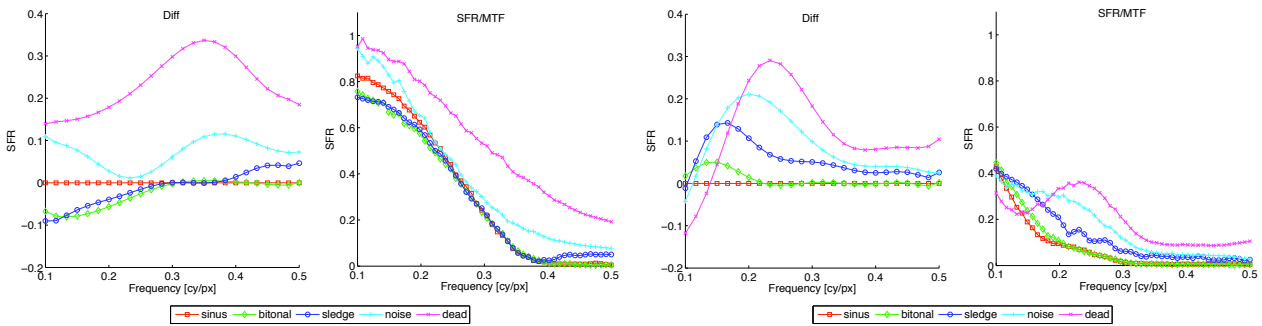


Figure 17. Comparison Nikon S1000pj, standard JPEG left: ISO100 right: ISO1600



Figure 18. Example image Nikon S1000pj. enlarged (4x), dead leaves target at ISO1600. The image content is covered by noise introduced by the camera's internal processing. Results in Figure 17. The results would lead to the conclusion, that the dead leaves MTF or Gaussian power spectrum is better than for the other methods, which is wrong.

5. CONCLUSION

- If no sharpening or denoising is applied to an image, all presented methods can describe the SFR (or MTF) of the system at low noise levels.
- Effects of image processing on a small range of spatial frequencies can only be seen if measured in the spatial domain (SFR-Siemens).
- The difference between SFR-Siemens.sinusoidal and SFR-Siemens.bitonal is low as long as sharpening is not applied.
- Denoising has low influence on SFR-Edge and SFR-Siemens, but significantly changes Dead Leaves MTF and Gaussian Power Spectrum.
- Sharpening is content depending, so different targets lead to different influence of the sharpening algorithms. This is the reason for variations in the transfer function using the related algorithms.
- Image noise has an influence on the Gaussian Power Spectrum method and an even larger influence on the Dead Leaves MTF method. If strong sharpening is applied to the image (and its noise content), the results derived from the dead leaves model get obscured by this.
- In general, the influence of de-noising can be described by the comparison of two methods to each other. The first provides a SFR measured on large structures, the second on randomly distributed, fine structures. SFR-Edge and Dead Leaves MTF would be one combination, SFR-Siemens and Gaussian Power Spectrum another. De-noising leads to a lower SFR measured on the smaller, fine details compared to the counterpart.
- The structures used for the first two methods are more influenced by sharpening algorithms than the second combination.
- Image noise can have such a huge impact on the results, that these fail to describe the de-noising in the camera.

REFERENCES

1. Artmann, Wueller, "Noise Reduction vs. Spatial Resolution", Electronic Imaging Conference, Proc. SPIE, Vol. 6817, 68170A (2008)
2. Artmann, Wueller, "Interaction of image noise, spatial resolution, and low contrast fine detail preservation in digital image processing", Electronic Imaging Conference, Proc. SPIE, Vol. 7250, 72500I (2009)
3. Phillips, Jin, Chen, Clark, "Correlating Objective and Subjective Evaluation of Texture Appearance with Applications to Camera Phone Imaging", Electronic Imaging Conference, Proc. SPIE, Vol. 7242, 724207 (2009)
4. Cao, Guichard, Hornung "Measuring texture sharpness", Electronic Imaging Conference, Proc. SPIE, Vol. 7250, 72500H (2009)
5. Loebich, Wueller, Klingen, Jaeger, "Digital Camera Resolution Measurement Using Sinusoidal Siemens Stars", Electronic Imaging Conference, SPIE Vol. 6502, 65020N (2007)
6. Uwe Artmann "Noise Reduction vs. Spatial Resolution", Diploma thesis at University of Applied Science Cologne Germany, downloadable via www.image-engineering.de
7. International Organization of Standardization, "ISO12233 Photography - Electronic still picture imaging - Resolution measurements"
8. Image Engineering, "White Paper: Camera Test", downloadable via: www.image-engineering.de
9. Williams, Wueller, Matherson, Yoshida, Hubel, "A Pilot Study of Digital Camera Resolution Metrology Protocols Proposed Under ISO 12233, Edition 2", Electronic Imaging Conference 2008, EI08_6808_3
10. D. Coffin, "Decoding raw digital photos in Linux", <http://www.cybercom.net/~dcoffin/dcraw/>
11. Loebich, Wueller, "Three Years of Practical Experience in Using ISO Standards for Testing Digital Cameras", IS&T/PICS Final Program and Proceedings, 2001, pp. 257-261.

12. Industrial International Imaging Association, Camera Phone Image Quality (CPIQ), www.i3a.org (ongoing work)
13. Bruno Klingen, "Fouriertransformation fuer Ingenieur- und Naturwissenschaften", Springer Verlag, 2001